

Note on the Electron Energy Spectrum in the Inner Van Allen Belt

G. PIZZELLA, C. D. LAUGHLIN, AND B. J. O'BRIEN

Department of Physics and Astronomy
State University of Iowa, Iowa City

NASw-17

Abstract. The energy spectrum of trapped electrons predicted by the neutron-albedo theory was tested experimentally with a magnetic electron spectrometer for the energy range $40 \leq E \leq 110$ kev. This detector was flown on the State University of Iowa radiation research satellite Injun I at an altitude of about 1000 km in the inner radiation zone over South America. Another detector on the same satellite measured the directional intensity of electrons with $E \geq 40$ kev. The data are consistent with a peak directional intensity of electrons in this region of $N(E) \sim 10^4 \exp(-E/160)$ particles $(\text{cm}^2 \text{ sec ster kev})^{-1}$, or with a power-law spectrum with a differential exponent of $-(1.0 \pm 0.2)$ for $40 \leq E \leq 110$ kev. This result is significantly in disagreement with the predictions of the neutron-albedo theory.

1. INTRODUCTION

The problem of determining the intensity and spectrum of electrons in the inner Van Allen zone has been considered by various authors [Van Allen, McIlwain, and Ludwig, 1959; Holly, Allen, and Johnson, 1961; McIlwain, 1961; and Weber, Lundquist, and Naumann, 1961]. However, there are formidable experimental difficulties in separating the electron component from the proton component, because of the high energies and hence high penetrability of shielding by the proton component. Therefore, although it is true that we know roughly the order of magnitude of the number of electrons in the inner zone, an accurate and complete electron spectrum has not yet been obtained.

One of the most important theoretical aspects of this problem is connected with the origin of electrons in the inner zone and with the origin of the inner zone itself. An important possible source for the particles trapped in the inner zone is the flux of albedo neutrons produced by cosmic rays. A recent work [Pizzella, McIlwain, and Van Allen, 1962] on the time variations of intensity in the inner belt has shown that such a weak source is not of dominant importance for particles of high energy:

protons $\gtrsim 18$ Mev
electrons $\gtrsim 1.1$ Mev

In this paper we study the low-energy electron component with the purpose of testing the neutron theory. Our further purpose will be to give

an electron spectrum, though quite roughly and over a limited energy range.

2. EXPERIMENTAL APPARATUS

For this study, data from detectors aboard the State University of Iowa radiation research satellite Injun 1 were used. The data were taken by the receiving stations of Quito, Lima, and Santos (South America), where Injun was at an altitude of about 1000 km.

For these stations, at this altitude, the ranges of L and B [McIlwain, 1961] covered were L from about 1.18 to about 1.4 earth radii, B from about 0.172 to about 0.21 gauss.

The time interval covered by the data was June 30, 1961, through January 1962.

The detectors used were the 213 Geiger tube; the three channels of the magnetic spectrometer (their characteristics are listed in Table 1); and the magnetometer, used as an aspect sensor for the directional detectors.

These detectors and methods of data transmission and analysis have been described in a study of the outer-zone electrons [O'Brien, Laughlin, Van Allen, and Frank, 1962].

3. ANALYSIS OF THE OBSERVATIONAL DATA

A. Definitions of Symbols

SpL, SpH, and SpB will indicate the counting rates of the low- and the high-energy channels and the background of the magnetic spectrometer.

TABLE 1. Injun Detectors Used in This Research

Detector	Symbol	Detectable Particles	Geometric Factor, cm ² ster
Anton type 213 Geiger tube	213	Electrons $E \gtrsim 40$ kev Protons $E \gtrsim 0.5$ Mev	1.5×10^{-2}
Spectrometer low-energy channel	SpL	Electrons $45 \lesssim E \lesssim 60$ kev	7.5×10^{-5}
Spectrometer high-energy channel	SpH	Electrons $80 \lesssim E \lesssim 110$ kev	6.5×10^{-5}
Spectrometer background monitor	SpB	Electrons $E \gtrsim 5$ Mev Protons $E \gtrsim 60$ Mev	[0.14 cm ²]
Magnetometer (aspect sensor)	Mag		

213 will indicate the counting rate of the 213 Geiger tube corrected for the dead time.

Mag will indicate the counting rate due to the magnetometer.

We shall make use also of the following quantities:

$$X_L = \text{SpL}/\text{SpB}$$

$$X_H = \text{SpH}/\text{SpB}$$

$$X_I = 213/\text{SpB}$$

The ratios are taken between data obtained at the same second of time.

The average of X_L data, for instance, will be indicated as \bar{X}_L . The median of the same data will be \tilde{X}_L .

B. Analysis of the Data

The greatest difficulty encountered in this analysis was to separate the low-energy electron component from the more penetrating high-energy electrons and protons, X rays, etc. The low-energy electrons, of course, can enter the detectors only through the front apertures, which have solid angles only a fraction of a steradian (Table 1). The penetrating component can enter over essentially 4π steradians. Thus discrimination of the low-energy electrons is possible only to the extent that their directional intensity in the direction in which the detectors are pointing is sufficient to give a significant portion of the counting rates compared with the rates due to the penetrating particles. From an inspection of SpL, SpH, and SpB the contribution of the low-energy electrons to these detectors can be seen to be very small. Furthermore, the spatial gradients in particle intensity in the inner zone are very strong, implying a strong dependency of

SpL, SpH, and SpB on the position in space. Finally, if a low-energy electron component exists, it will depend on the angular position of the directional detectors with respect to the lines of force of the earth's magnetic field. This angular position is measured by Mag. (The value of Mag is about 115 when the detector is perpendicular to the field line of force.) Therefore the variables on which the low-energy electron component of the counting rates will depend are three: L , B , and Mag. The high-energy component will depend on L and B (we are forced to ignore time as a parameter in order that the statistical accuracy be the maximum possible).

In spite of the large number of measurements (about 30,000) it is not possible to have results statistically meaningful if all the three variables above are considered. Therefore we will not consider the dependency of the low-energy electron component on L and B . The quantities X_L , X_H , and X_I , as above defined, are introduced for the following reason. Suppose that the contribution to SpL, for instance, is due to the low-energy electrons, $(\text{SpL})_E$, and to the more penetrating particles, $(\text{SpL})_B$, that is:

$$\text{SpL} = (\text{SpL})_E + (\text{SpL})_B$$

Then we define

$$X_L = [(\text{SpL})_E + (\text{SpL})_B]/\text{SpB}$$

If $(\text{SpL})_B$ is proportional to SpB and if $(\text{SpL})_E \ll (\text{SpL})_B$, then X_L will be constant for every value of the parameters L , B , Mag. If $(\text{SpL})_E$ is not negligible compared with $(\text{SpL})_B$, the quantity X_L will be a function of L , B , Mag. The dependency with L and B of X_L will involve the dependency of $(\text{SpL})_E$ and $(\text{SpL})_B$ and pre-

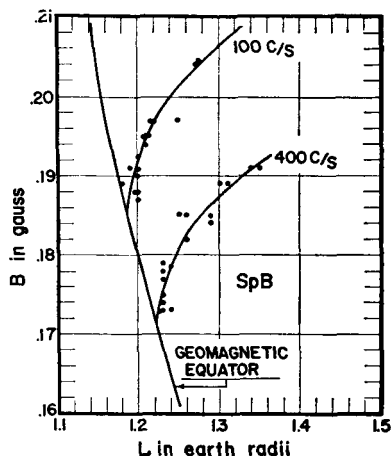


Fig. 1. Contours of constant counting rate, SpB, of the spectrometer background. The two curves at 100 and 400 c/s delineate the region in the L, B plane in which the data are taken.

sumably will be very complicated. The dependency with Mag must be such that, if electrons contribute significantly, X_L has a maximum when the detector is perpendicular to the field, that is, when $\text{Mag} = 115$.

The analysis will be performed as follows: (1) ignore the B and L dependency; (2) concentrate on the Mag dependency; and (3) assume that $(\text{SpL})_B \propto (\text{SpH})_B \propto (\text{SpB})$. Since the B, L dependency does exist, we must examine a very large amount of data for each value of Mag.

C. Selection of Data

We call a set of observational data a set of observations performed simultaneously with the five detectors SpL, SpH, SpB, 213, and Mag. Not all sets available from Injun will be taken, but only those for which SpB is greater than 100 c/s and smaller than 400 c/s. Also we will consider only the sets for which $75 \leq \text{Mag} < 155$. The reasons for the SpB selection are:

1. We do not want very small counting rates, because they have greater statistical errors.

2. If we wish to give an estimation of the absolute values of the intensities we need to know the value of SpB. In fact, with the introduction of X_L, X_H , and X_I we refer all the detectors to SpB.

3. Finally, such a selection of SpB also restricts the allowed ranges of L and B , because

it forbids us to go in regions where the counting rate SpB is extremely high or extremely low. It therefore minimizes spatial effects. This selection is illustrated in Figure 1.

D. Results

The dependence of $\bar{X}_L, \bar{X}_L, \bar{X}_H, \bar{X}_H, \bar{X}_I$, and \bar{X}_I on Mag is shown in Figure 2. The above quantities were calculated as follows:

1. Select the sets of data in groups according to intervals of Mag 10 c/s wide.
2. Make the frequency distributions of the values X_L, X_H , and X_I for each group ($\text{Mag} \pm 5$).
3. Calculate the averages and the medians for each ($\text{Mag} \pm 5$). In Figure 3 the frequency distributions are shown. In Table 2 the averages and the medians are tabulated together with the number of data used in each determination and the values of Mag.

From Figure 2 the three maximums do not appear to be at the same value of Mag. This can be ascribed to some statistical fluctuation

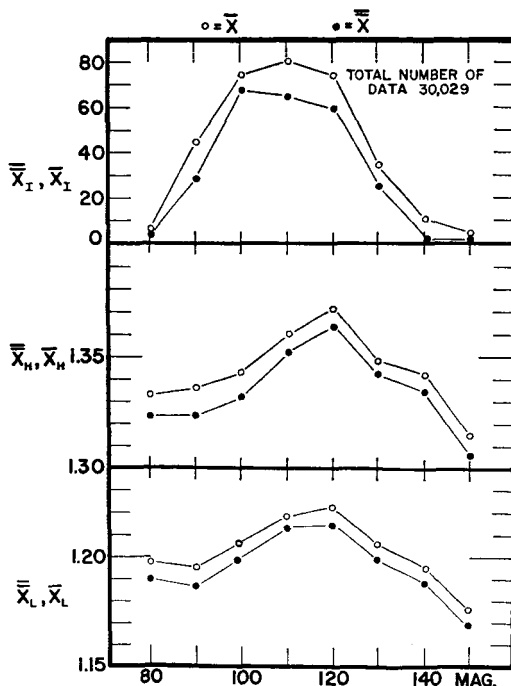


Fig. 2. Effect of the angular position with respect to the field lines, Mag, on the 213 Geiger counter and on the two channels of the magnetic spectrometer.

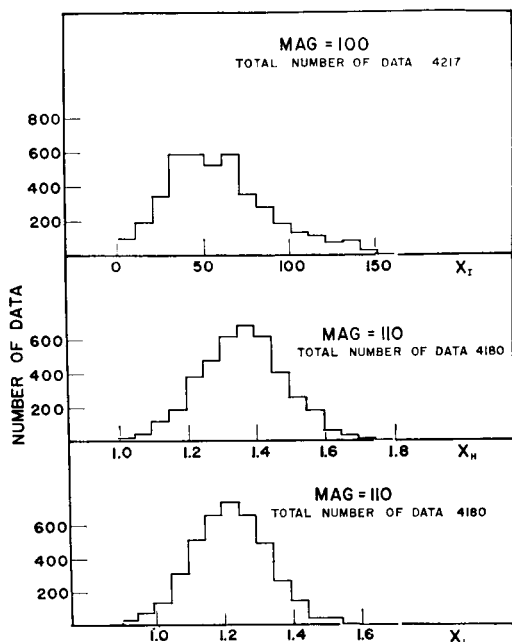


Fig. 3. Frequency distributions of the quantities \bar{X}_I , X_H , X_L at a fixed value of the parameter Mag.

and/or to a little difference in the geometrical arrangement of the detectors.

In Figure 4 we have plotted \bar{X}_H , \bar{X}_L against \bar{X}_I , \bar{X}_L , taking the points from Table 2. Note the remarkably good correlation shown in this figure between X_H and X_L . It is, in fact, our first check that the detected effect shown in Figure 2 is not instrumental.

4. DETERMINATION OF THE ELECTRON ENERGY SPECTRUM

A. Interpretation of the Experimental Results

From Figure 2 we can conclude that the low-energy electrons in the inner zone are numerous enough to activate the Geiger counters in the magnetic spectrometer of Injun 1. The dependency of \bar{X}_I on Mag is so strong that there are no doubts that for Mag = 110 the 213 Geiger tube is counting low-energy particles, dominantly electrons with energy above 40 kev [Frank, Dennison, and Van Allen, 1962]. Since for X_L and X_H the variation with Mag is only about 3 per cent, we must carefully verify that such effect is due to low-energy electrons. The verification will be supplied later by the good agree-

ment shown with the other experiments and by the internal consistency of the final results. Thus we shall assume that the variation shown in Figure 2 is due to the low-energy component for \bar{X}_L , \bar{X}_H , and \bar{X}_I .

The response of the spectrometer is sufficient for determining an electron spectrum in which there are only two unknowns. For this purpose we shall make use mainly of the result shown in Figure 4.

We observe that the linear relationship shown in this figure is not very much affected by the choice between the medians and the averages. This relationship is expressed by

$$X_H = 1.21 \times X_L - 0.11 \quad (1)$$

where we do not distinguish between averages and medians. We define the following quantities:

$$\begin{aligned} X_H &= X_{H0} + X_{HE} \\ X_L &= X_{L0} + X_{LE} \end{aligned} \quad (2)$$

$$r = X_{LE}/X_{HE}$$

where X_{H0} , X_{L0} represent the contribution to X_H , X_L due to the penetrating component; X_{HE} , X_{LE} represent the contribution due to the low-energy electron component. These two quantities will be functions of the angular position, expressed by Mag.

The electron spectrum which we shall determine will be based on the hypotheses that (a) the spectrum does not depend on the angular orientation (this means that we assume r to be independent of Mag) and (b) X_{L0} , X_{H0} are independent of Mag.

With these assumptions we can consider the variations dX_{HE} , dX_{LE} due to a variation in Mag, and we have

$$r = dX_{LE}/dX_{HE}$$

From (1),

$$dX_H = 1.21 dX_L$$

From (2),

$$dX_L = dX_{LE} \quad dX_H = dX_{HE}$$

and thus we get

$$r = 1/1.21$$

It is now possible to compute the ratio of the soft component measured by the high-energy

TABLE 2. Experimental Results

Mag	\bar{X}_L	\bar{X}_L	\bar{X}_H	\bar{X}_H	\bar{X}_I	\bar{X}_I	Number of Data
80	1.191	1.199	1.324	1.331	3	16	4189
90	1.187	1.196	1.324	1.336	28	45	4161
100	1.199	1.208	1.332	1.344	68	75	4217
110	1.214	1.219	1.352	1.360	65	81	4180
120	1.215	1.223	1.364	1.372	60	75	4203
130	1.199	1.206	1.342	1.349	26	35	3677
140	1.189	1.197	1.335	1.343	2	11	2978
150	1.169	1.176	1.306	1.316	2	5	2424
Total number of data						30,029	

channel to the soft component measured by the low-energy channel of the magnetic spectrometer. If the directional geometrical factors, as given in Table 1, are considered, we have

$$R = \frac{(\text{SpL})_E}{(\text{SpH})_E} = \frac{1}{1.21} \frac{6.5}{7.5} = 0.72$$

B. Determination of the Electron Energy Spectrum

Present knowledge of the electron spectrum in the inner zone suggests that the spectrum function has the following characteristics: (a) It is not a strongly varying function at low energies; (b) it drops down very quickly at high energies (about 1 Mev); and (c) the total energy carried by all the electrons with energy above 1 keV must be less than 2-3 ergs/(cm² sec ster) [Freeman, 1962] at the Injun altitudes and regions treated here.

We propose to represent such a spectrum with

an exponential function. In other words, for the differential energy spectrum we propose

$$N(E) dE = N_0 e^{-E/E_0} dE$$

This function meets the above three specifications and is of very simple mathematical form. No other reasons for its choice are advocated.

The two parameters N_0 and E_0 can be determined by using SpL and SpH, above. We have

$$(\text{SpL})_E = \int_0^\infty E_L(E) N(E) dE$$

$$(\text{SpH})_E = \int_0^\infty E_H(E) N(E) dE$$

where $E_L(E)$ and $E_H(E)$ represent the efficiencies for the two channels of the spectrometer. For the low channel, $E_L(E)$ is about unity over a width of about 15 keV, and then drops to zero. For the high channel the width of $E_H(E)$ is about 30 keV. If we perform the two integrals making use of the measured values of $E_L(E)$ and $E_H(E)$ we get a relationship between R and E_0 .

In our case, it is $R = 0.72$ and then $E_0 = 160$ keV. The value of E_0 is correct within a factor of 2 (provided that the earlier interpretation of the data is correct). N_0 can be determined in the following way. When the spectrometer is perpendicular to the magnetic field direction and hence facing into the maximum directional intensity, we have a maximum value of \bar{X}_L around 1.22 (see Figure 2). Also we have a minimum value for \bar{X}_L around 1.18. This gives

$$(\text{SpL})_E = (1.22 - 1.18)$$

× SpB/ geometric factor

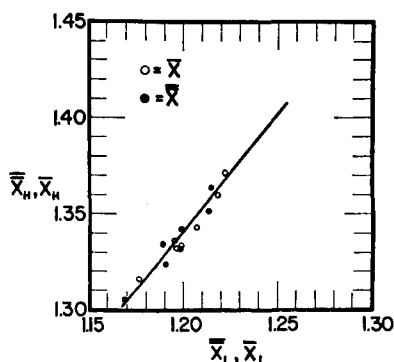


Fig. 4. Correlation between the two channels of the magnetic spectrometer. The slope of the straight line determines the exponent in our exponential electron spectrum for the inner zone.

and similarly

$$(\text{SpH})_E = (1.37 - 1.32)$$

$$\times \text{SpB/geometric factor}$$

That is:

$$(\text{SpL})_E = 520 \times \text{SpB}$$

$$(\text{SpH})_E = 770 \times \text{SpB}$$

The value of SpB is strongly dependent on the position in space. To increase the statistical accuracy, we have accepted data from $100 \leq \text{SpB} \leq 400$. The average value of SpB is 250 c/s.

To obtain the number of electrons/cm² sec ster kev, we must consider the energy widths of the two channels in the spectrometer. Because of the rough determination of SpB it is sufficient to take 15 kev and 30 kev for the two widths (low and high channels), assuming rectangular spectral passbands. Finally,

$$\begin{aligned} N(51 \text{ kev}) &= \frac{520 \cdot 250}{15} \\ &= 8100 \frac{\text{electrons}}{\text{cm}^2 \text{ sec ster kev}} \end{aligned}$$

$$\begin{aligned} N(91 \text{ kev}) &= \frac{770 \cdot 250}{30} \\ &= 6400 \frac{\text{electrons}}{\text{cm}^2 \text{ sec ster kev}} \end{aligned}$$

in the perpendicular direction. Thus the differential energy spectrum for electrons in the inner zone will be

$$N(E) \simeq 10^4 e^{-E/160} \frac{\text{electrons}}{\text{cm}^2 \text{ sec ster kev}}$$

with the energy E expressed in kev. This result is in reasonable agreement with the measurements of *Holly, Allen, and Johnson* [1961].

The spectrum above was obtained without making any use whatsoever of data from the 213 Geiger tube. Therefore the first check can be made by integrating the spectrum for energies greater than 40 kev. We have for the *predicted* flux of electrons measured by the 213 Geiger tube

$$\begin{aligned} (213)_E &= \int_{40 \text{ kev}}^{\infty} N(E) dE = 160 \cdot 10^4 e^{-40/160} \\ &= 1.3 \cdot 10^6 \frac{\text{electrons}}{\text{cm}^2 \text{ sec ster}} \end{aligned}$$

from our experiment (Figure 2); we have, in the perpendicular direction, the flux *measured* by the 213 Geiger tube

$$(213)_E = \frac{80 \cdot 250}{1.5 \cdot 10^{-2}} = 1.3 \cdot 10^6 \frac{\text{electrons}}{\text{cm}^2 \text{ sec ster}}$$

if we take the maximum of X_i equal to 80.

It must be pointed out that this check is independent of SpB, because SpB appears as a factor in both the theoretical and the experimental determinations. The agreement is extremely good. Note that this is not a verification of the tentative spectral form, since a differential power-law spectrum with an exponent of about (-1.0 ± 0.2) would also be consistent with the 213 data. The important fact is that the agreement justifies our earlier assumption that the 3 per cent increase in X_L and X_H at Mag about 115 (Figure 2) was due to electrons with energies within the spectrometer passbands and with pitch angles of about 90°. Finally, we compute the total energy carried by the electrons. We have

$$E_{\text{tot}} = \int_0^{\infty} EN(E) dE = 2.5 \cdot 10^8 \frac{\text{kev}}{\text{cm}^2 \text{ sec ster}}$$

$$E_{\text{tot}} = 0.4 \frac{\text{ergs}}{\text{cm}^2 \text{ sec ster}}$$

This value satisfies the requirements of section 4B.

5. COMPARISON WITH THE NEUTRON-ALBEDO THEORY

The present data disagree with predictions of the neutron-albedo theory. Considering the different energy widths in the two spectrometer channels we have a ratio of the differential energy spectrum at 51 kev and 91 kev of 1.3. From *Lenchek, Singer, and Wentworth* [1961], at an altitude of 1100 km and for $L = 1.5$ we would predict from the albedo-neutron theory a ratio of about 0.4. And so we have a discrepancy of a factor of 3. Also from the theory we can get the ratio

$$\begin{aligned} &\frac{\text{Number of electrons with energy greater than 40 kev}}{\text{Number of electrons/kev at 50 kev}} \\ &= 1300 \text{ kev} \end{aligned}$$

From our experiment the ratio is

$$(1.3 \cdot 10^6)/(8.1 \cdot 10^3) = 160 \text{ kev}$$

Thus for this case we have a discrepancy of a factor of 8.

The conclusion from an examination of these data is that the neutron-albedo theory as now developed cannot be the dominant source of electrons with $40 \lesssim E \lesssim 110$ kev in the inner radiation zone. As is shown elsewhere [Pizzella, McIlwain, and Van Allen, 1962], it also cannot be the dominant source of the penetrating high-energy protons.

Acknowledgments. We are very appreciative of stimulating discussions with Dr. J. A. Van Allen, Mr. J. Freeman, and Mr. L. Frank. The students who did such excellent work in building Injun 1 included W. Whelpley, D. Gurnett, D. Stilwell, and R. Trachta. We thank Mr. Roger Tetrick of Goddard Space Flight Center and Dr. G. Pieper of the Applied Physics Laboratory of the Johns Hopkins University for assistance with telemetry reception in South America.

This work was supported in part by the Office of Naval Research under contract N9onr93803.

REFERENCES

- Frank, L. A., D. C. Dennison, and J. A. Van Allen, Electrons in the earth's inner radiation zone, abstract, *J. Geophys. Research*, **67**, 3558, 1962.
- Freeman, J. W., Detection of an intense flux of low-energy protons or ions trapped in the inner radiation zone, *J. Geophys. Research*, **67**, 921-929, 1962.
- Holly, F. E., L. Allen, Jr., and R. G. Johnson, Radiation measurements to 1500 kilometer altitude at equatorial latitudes, *J. Geophys. Research*, **66**, 1627-1639, 1961.
- Lenchek, A. M., S. F. Singer, and R. C. Wentworth, Geomagnetically trapped electrons from cosmic ray albedo neutrons, *J. Geophys. Research*, **66**, 4027-4047, 1961.
- McIlwain, C. E., Evidence of high fluxes of electrons in the inner zone, abstract, *J. Geophys. Research*, **67**, 1647, 1962.
- McIlwain, C. E., Coordinates for mapping the distribution of magnetically trapped particles, *J. Geophys. Research*, **66**, 3681-3691, 1961.
- O'Brien, B. J., C. D. Laughlin, J. A. Van Allen, and L. Frank, Measurements of the intensity and spectrum of electrons at 1000 km altitude and high latitudes, *J. Geophys. Research*, **67**, 1209-1226, 1962.
- Pizzella, G., C. E. McIlwain, and J. A. Van Allen, Time variation of intensity in the earth's inner radiation zone, October 1959 through December 1960, *J. Geophys. Research*, **67**, 1235-1254, 1962.
- Van Allen, J. A., C. E. McIlwain, and G. H. Ludwig, Radiation observations with satellite 1958e, *J. Geophys. Research*, **64**, 271-286, 1959.
- Weber, A. H., C. A. Lundquist, and R. J. Naumann, Directional flux densities and mirror-point distribution of geomagnetically trapped charged particles from satellite 1958e measurements, abstract, *J. Geophys. Research*, **67**, 1662, 1962.

(Manuscript received May 28, 1962.)